Regular Article

PHYSICAL CHEMISTRY RESEARCH
Published by the
Iranian Chemical Society
www.physchemres.org
info@physchemres.org

Phys. Chem. Res., Vol. 10, No. 1, 1-12, March 2022
DOI: 10.22036/PCR.2021.271462.1881

The Effects of Silicon Oxide on the Structure, Physical Chemistry Properties, and Bioactivity of Phosphate Glasses Containing Sodium, Strontium, and Titanium Oxides

I. EL Abdouni[a], S. Krimi[a,*] and H. Oudadesse[b]

[a]*Laboratory of Physical Chemistry of Inorganic Materials (LPCMI), Faculty of Sciences Ain chock, University of Hassan II Casablanca, Morocco*

[b]*University of Rennes, CNRS, ISCR-UMR 6226, F-35000 Rennes, France*

(Received 2 February 2021, Accepted 19 July 2021)

Glasses with molar compositions $40Na_2O$-10SrO-(20-x)TiO_2-xSiO_2-$30P_2O_5$ ($0 \leq x \leq 10$; O/P = 4), were prepared by the classical melt-quenching technique and structurally characterized by X-ray diffraction (XRD), differential scanning calorimetry (DSC), Fourier transform infrared (FTIR), Raman, nuclear magnetic resonance (NMR), and density measurements. The introduction of SiO_2 into the phosphate glass slightly weakened the glass network, as shown by the small increase in the molar volume (V_M) and the decrease in the glass transition temperature (T_g). This behavior was due to the existence of more ionic P-O-Si than P-O-P bonds. Spectroscopic studies showed that SiO_2, like P_2O_5 oxide, behaved as a network former and that the glass structure contained P-O, P-O-P, Si-O, Si-O-Si, Ti-O, Ti-O-Ti, P-O-Ti, and P-O-Si linkages. The preliminary results of the *in vitro* bioactivity tests showed the existence of ionic exchanges between the simulated body fluid (SBF) solution and the studied glasses. X-ray powder diffraction and FTIR spectroscopy confirmed the formation of the Ca-P layer on the surfaces of the tested compositions.

Keywords: Phosphate, Glass, Bioactivity, Raman, NMR

INTRODUCTION

Phosphate glasses have attracted great interest in recent years due to their chemical properties and numerous applications in various fields, such as energy, health, environment, and catalysis [1-4]. One of the properties of phosphate glasses is that they have the potential to be used as biomaterials because of their chemical composition and low chemical durability [5]. In view of the great need for bioactive materials, different phosphate glass compositions have been investigated [6-10]. Understanding the structure of phosphate glasses is of fundamental interest to chemists because it allows them to adjust compositions to the targeted application. Various elements of the periodic table have been incorporated into different phosphate glass compositions to improve their chemical, physical, and biological properties [11-13]. The diverse properties and applications of phosphate glasses depend on their structure; phosphate groups are classified according to the Q^n nomenclature, where n varies from 0 to 4 and represents the number of bridging oxygen (BO) atoms per phosphate tetrahedron. The Q^n-groups notation is related to the oxygen-to-phosphorus ratio. Thus, the glass structure can be formed by a cross-linked network of Q^3 tetrahedra (O/P = 2.5) and infinite chains of Q^2 tetrahedra (O/P = 3), or by a small diphosphate Q^1 (O/P = 3.5) and monophosphate Q^0 (O/P = 4) [14]. In this regard, many studies have been conducted on the effect of titanium or/and strontium oxides on sodium phosphate glasses [15-17]. The coordination number of Ti^{4+} ions in the glasses was found to be four, five, or six [18,19]. Furthermore, titanium- and strontium-

*Corresponding author. E-mail: saida.krimi@etu.univh2c.ma

doped phosphate-based glasses were found to exhibit interesting physicochemical and biocompatibility properties, making them promising candidates for use as substitute biomaterials [20]. A study on the effect of SiO_2 and Fe_2O_3 on the surface properties of phosphate-based glasses showed that the synthesized composites were cytocompatible and that the cells were aligned along the phosphate glass fibers in the composite material [21]. Substituting TiO_2 for SiO_2 improved the physical properties and biocompatibility of the P_2O_5-CaO-Na_2O glass system [22]. Recently, the effect of silica on the structural and luminescence properties of Eu^{3+}/Tb^{3+} co-doped phosphate glass (P_2O_5-CaO-Na_2O) has been reported [23].

To the best of our knowledge, the use of silicon oxide in phosphate glass matrix for biological applications has scarcely been reported in the literature. Accordingly, the present study aimed to investigate the effect of replacing titanium with silicon in sodium phosphate glasses containing strontium and study the *in vitro* biological behavior in the SBF solution for the obtained glasses.

MATERIALS AND METHODS

Glasses with molar compositions $40Na_2O$-10SrO-(20-x) TiO_2-xSiO_2-$30P_2O_5$ ($0 \leq x \leq 10$) were prepared in air by melt-quenching of the mixture of reagent grade chemicals of Na_2CO_3 (99%), $SrCO_3$ (98%), TiO_2 (99%), SiO_2 (99%), and $(NH_4)_2HPO_4$ (99%). The mixtures were heated in a platinum crucible at 200 °C, 400 °C, and 600 °C for 12 h to decompose phosphate and carbonate reagents. The temperature was then progressively increased until complete melting occurred at temperatures between 1100 °C and 1250 °C depending on the silicon oxide content. Then, the melts were poured onto a metallic plate preheated at 150 °C. All the obtained glasses were annealed at T_g-20 °C, to remove residual stresses, and T = 640 °C. Figure 1 shows photographs of the glasses prepared under the conditions described above. As it can be seen, all the glasses were colorless and transparent. The obtained glasses $40Na_2O$-10SrO-(20-x) TiO_2-xSiO_2-$30P_2O_5$ were denoted as PSi0 (x = 0), PSi2 (x = 2), PSi4 (x = 4), PSi6 (x = 6), PSi8 (x = 8), and PSi10 (x = 10).

X-ray diffraction (XRD) was used to confirm the amorphous state of the synthesized materials and identify

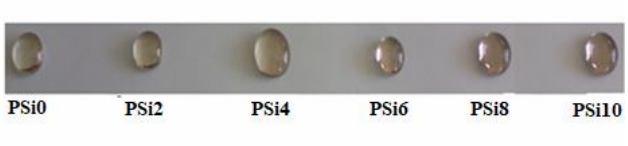

Fig. 1. Photographs of $40Na_2O$-10SrO-(20-x)TiO_2-xSiO_2-$30P_2O_5$ ($0 \leq x \leq 10$) glasses.

the crystalline phases. XRD patterns were recorded at room temperature using the D8-Advance diffractometer (Bruker) with Cu Kα radiation in the 2θ range from 10° to 60°. Glass transition, crystallization, and melting temperatures (T_g, T_c, and T_m, respectively) were measured on 50 mg of samples under N_2 gas atmosphere at 0.1 MPa without pressure control using a Setaram Labsys 1600TG-DTA/DSC thermal analyzer with a heating rate of 10 °C min^{-1} and a measurement error of 5 °C in a platinum crucible. To obtain more information about the structure of the obtained glasses, their powders were analyzed by Raman, Fourier transform infrared (FTIR), and nuclear magnetic resonance (NMR) spectroscopies. Raman spectra were obtained using a Vertex 70 spectrometer in the spectral range of 400-3600 cm^{-1} with a laser source (λ = 633 nm). FTIR analysis was performed using IR Affinity-1S spectrometer (Shimadzu) from 400 to 4000 cm^{-1}. ^{31}P MAS NMR data were collected at 12 kHz on a Bruker Advance 600 MHz spectrometer. The density (ρ) was measured on bulk glasses by the Archimedes method and using diethyl phthalate as the immersion liquid. Glass density (ρ) was measured using the following equation: $\rho = [m_a/(m_a - m_l)]\rho_l$, where m_a is the mass of the sample in air, m_l is the mass of the sample immersed in the liquid, and ρ_l is the density of the liquid (diethyl phthalate) at room temperature. The precision of the measurements was about ± 0.02 g cm^{-3}. Molar volume was calculated using the relation $V_M = M/\rho$, in which M is the molar mass of the glass and ρ is the density). The *in vitro* bioactive behavior of the studied glasses was evaluated by dissolving 30 mg of powder in 60 ml of the SBF having the same composition as the blood plasma. The samples were immersed for 30 days at 37 °C and 50 rpm min^{-1} to allow a similar physiological environment. The SBF solution was prepared, as previously described [24], by dissolving the following chemical reagents in deionized water: NaCl, $NaHCO_3$, $(CH_2OH)_3{\cdot}CNH_2$, KCl, $CaCl_2{\cdot}2H_2O$, KH_2PO_4,

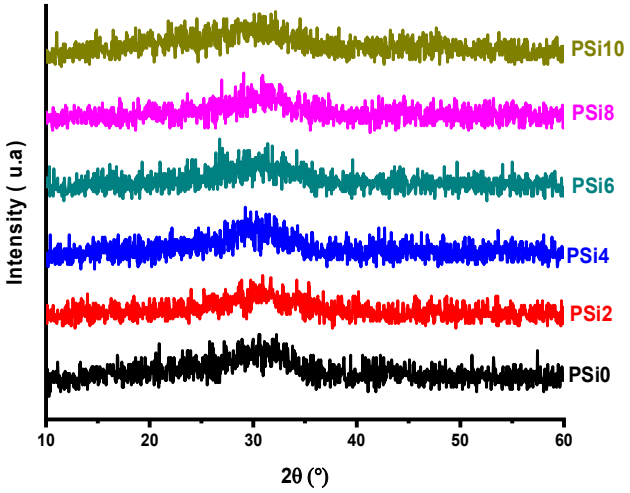

Fig. 2. X-ray diffraction of $40Na_2O$-$10SrO$-$(20-x)TiO_2$-$xSiO_2$-$30P_2O_5$ ($0 \leq x \leq 10$) glasses.

and $MgCl_2 \cdot 6H_2O$. The pH of the solution was adjusted to 7.4 by 6 N HCl.

After immersion, the samples were washed with ethanol and dried at room temperature for 24 h. Dried glass powders were analyzed by means of X-ray powder diffraction and FTIR spectroscopy to determine the structural changes that occurred on the surface of glass samples after reacting with the SBF solution.

RESULTS AND DISCUSSION

X-Ray Diffraction (XRD) Characterization

XRD patterns of $40Na_2O$-$10SrO$-$(20-x)TiO_2$-$xSiO_2$-$30P_2O_5$ glasses ($0 \leq x \leq 10$) are shown in Fig. 2. The absence of diffraction peaks indicates the amorphous state of all the prepared materials. All the obtained phosphate glasses were heated at T = 640 °C for 12 h. The identified crystalline phases from the annealed glasses are shown in Fig. 3. XRD diffractogram of the silicon-free glass composition with the chemical formula $Na_4Sr_{0.5}Ti(PO_4)_3$ showed the crystallization of the phosphate phases $Na_5Ti(PO_4)_3$ (ASTM powder diffraction file, N°01-081-2420), $NaTi_2(PO_4)_3$ (ASTM powder diffraction file, N°01-084-2009), and the diphosphate phase $Sr_2P_2O_7$ (ASTM powder diffraction file, N°00-024-1011). For the glass

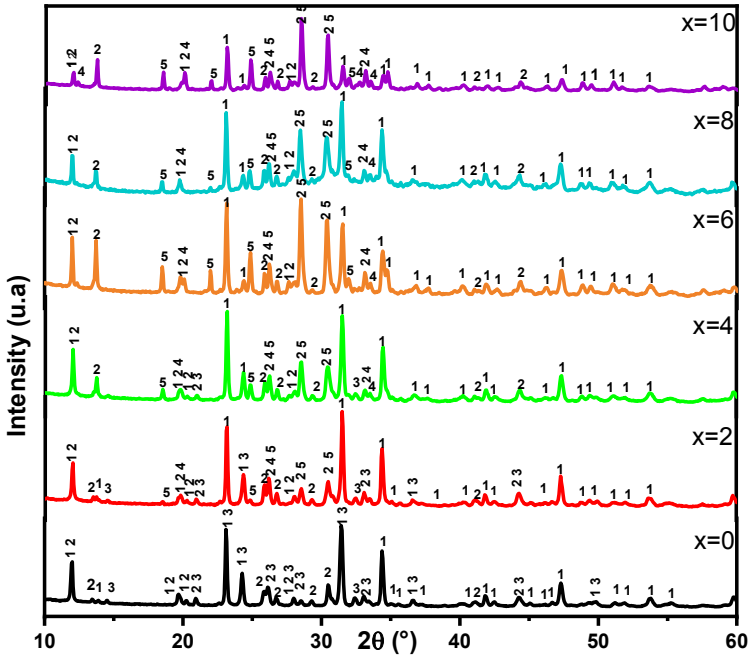

Fig. 3. X-ray diffractograms of $40Na_2O$-$10SrO$-$(20-x)TiO_2$-$xSiO_2$-$30P_2O_5$ ($0 \leq x \leq 10$) glasses heated at T = 640 °C [(1) $Na_5Ti(PO_4)_3$, (2) $Sr_2P_2O_7$, (3) $NaTi_2(PO_4)_3$, (4) $Na_4P_2O_7$, (5) SiO_2].

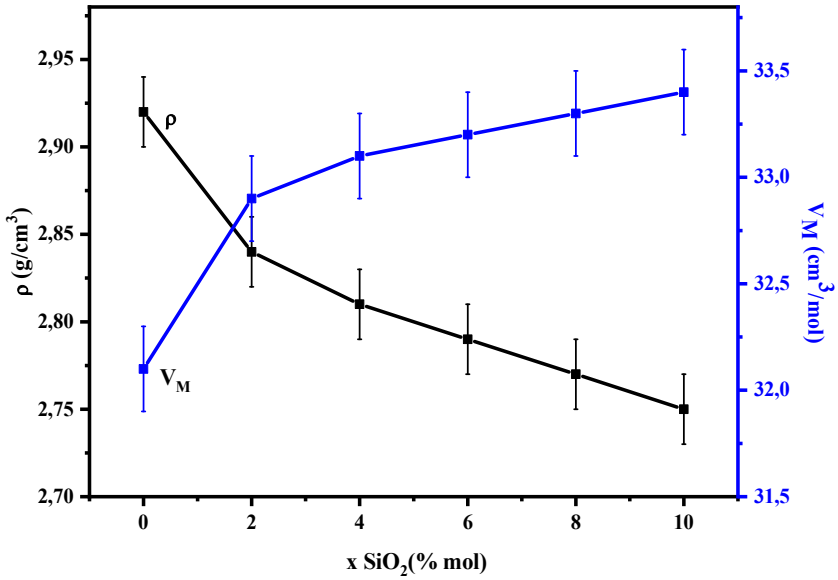

Fig. 4. The evolution of density and molar volume for $40Na_2O$-10SrO-(20-x)TiO_2-xSiO_2-$30P_2O_5$ ($0 \leq x \leq 10$) glasses *versus* SiO_2 mol%.

Table 1. Compositions, Molar Mass, Density, Molar Volume, and Characteristic Temperatures of the Studied Glasses

	Na_2O (mol%)	SrO (mol%)	TiO_2 (mol%)	SiO_2 (mol%)	P_2O_5 (mol%)	M (g mol^{-1})	ρ (g cm^{-3}) (± 0.02)	V_M (cm^3 mol^{-1}) (± 0.2)	T_g (°C) (± 5)	Tc (°C) (± 5)	T_m (°C) (± 5)
PSi0	40	10	20	0	30	93.71	2.92	32.1	440	560/580	704
PSi2	40	10	18	2	30	93.32	2.84	32.9	435	563/585	704
PSi4	40	10	16	4	30	92.92	2.81	33.1	425	560/577	704
PSi6	40	10	14	6	30	92.52	2.79	33.2	410	563	674/723
PSi8	40	10	12	8	30	92.13	2.77	33.3	400	553/563	678/720
PSi10	40	10	10	10	30	91.73	2.75	33.4	387	550/577	683/720

compositions containing SiO_2, XRD patterns revealed the existence of the previous phases crystallized from the composition x = 0 in addition to SiO_2 (ASTM powder diffraction file, N°01-070-3318) and $Na_4P_2O_7$ (ASTM powder diffraction file, N°00-010-0187).

Density and Molar Volume

Figure 4 shows the variation in the density (ρ) and molar volume (V_M) *versus* SiO_2 content of the studied glasses. It can be clearly seen that the value of the density decreased from 2.92 to 2.77 while the molar volume increased from 32.1 to 33.4 cm^3 mol^{-1} when the percentage of SiO_2 in the glass increased from 0 to 10 mol% (Table 1). The decrease observed in the density of the glasses when titanium oxide TiO_2 was replaced with silicon oxide SiO_2 can be attributed to the fact that the molecular weight of silicon oxide (60.08 g mol^{-1}) is lower than that of titanium oxide (79.87 mol^{-1}). The molar volume ($V_M = M/\rho$) is inversely

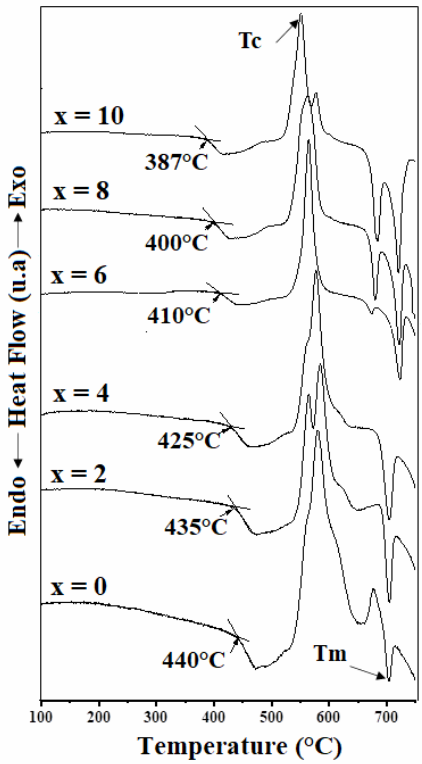

Fig. 5. DSC thermograms of $40Na_2O$-10SrO-(20-x)TiO_2-xSiO_2-30P_2O_5 ($0 \leq x \leq 10$) glasses.

proportional to the density (ρ), so every decrease in ρ implies an increase in V_M. At the same time, the molar mass (M) values of the studied glasses decreased from 93.71 to 91.73 mol^{-1}, suggesting that the molar volume must have decreased as well. These two antagonist effects led to a slight variation in the molar volume when the SiO_2 content increased in the glass matrix. Typical behavior was observed in other phosphate glasses [22].

Differential Scanning Calorimetry (DSC) Characterization

Figure 5 shows the DSC thermograms of the $40Na_2O$-10SrO-(20-x)TiO_2-xSiO_2-30P_2O_5 glasses ($0 \leq x \leq 10$). All the prepared glasses exhibited an endothermic deviation due to the glass transition temperature (T_g), followed by exothermic peaks due to the crystallization temperatures (T_c) and endothermic changes due to the melting temperatures (T_m) of the crystalline phases. The values of characteristic temperatures (Tg, Tc, Tm) for the studied glasses are summarized in Table 1. Tg was determined as the inflection point of the first endothermic peak, Tc as the maximum of the exothermic peaks, and Tm as the minimum of the second endothermic peak. According to Fig. 5, the DSC curves for some glass compositions showed more than one peak of T_c and T_m, suggesting the crystallization of a mixture of phases and the uniqueness of the crystallization and melting temperatures of each phase. This result is in good agreement with the results of XRD characterization.

The T_g value decreased from 440 °C for x = 0 to 387 °C for x = 10, suggesting that the introduction of SiO_2 oxide into the glass composition weakened the vitreous network. This result is in good agreement with the increase observed previously in the molar volume. The observed decrease in

Table 2. Raman Band Assignments of the Studied Glasses

Wavenumbers ν (cm^{-1})	Assignments	Ref.
400-600	O-Si-O Angle deformation O-Ti-O Angle deformation O-P-O bending modes P-O-P deformations	[25,30,41]
630-800	P-O-P (Q^1) stretching symmetric Si-O-Si (Q^1) bond stretching vibration Ti-O-Ti-O chains Ti-O vibrations of TiO_6 octahedra	[29,31-40]
800-1100	$(PO_4)^{3-}$(Q^0) symmetric stretching $(SiO_4)^{4-}$(Q^0) asymmetric stretching P-O-P (Q^1) asymmetric stretching	[30-35]
1150	P-O-Si (Q^1) stretching vibration P-O in (PO_2) sym	[14,29,31]

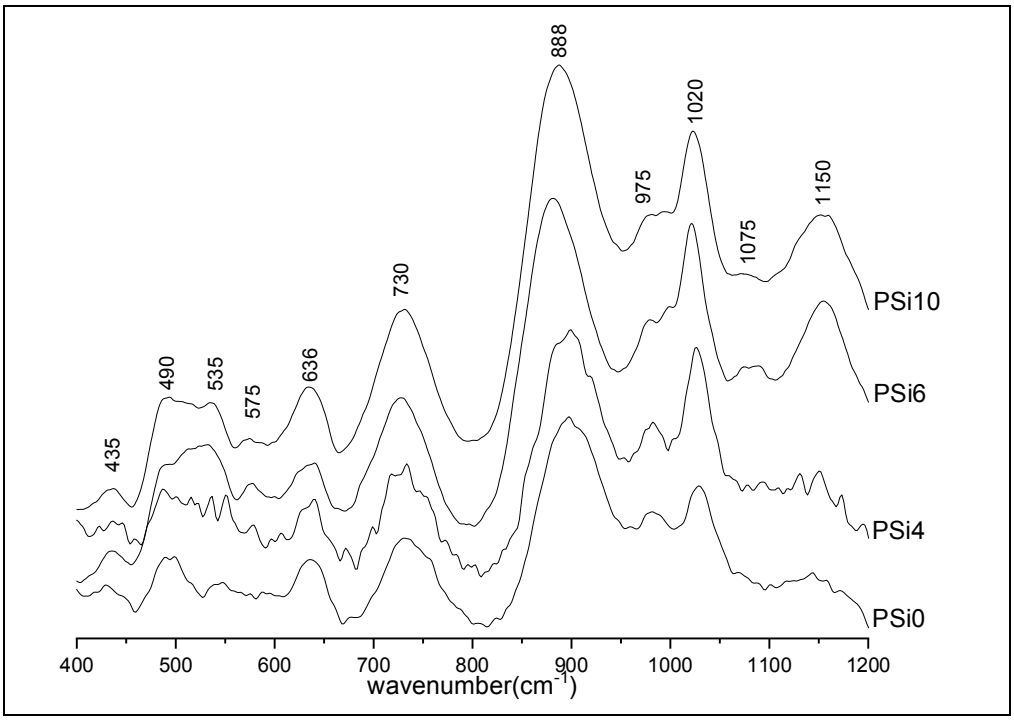

Fig. 6. Raman spectra of 40 Na_2O-10SrO-(20-x)TiO_2-xSiO_2-30P_2O_5 ($0 \leq x \leq 10$) glasses.

the glass transition temperature (T_g) indicates that the P-O-Si bonds must have been less covalent than the P-O-P bonds in the glass network. Therefore, it can be concluded that SiO_2 oxide, together with P_2O_5 oxide, acted as a network former in the studied glasses. Similar results have been observed in other phosphate glasses [26-28].

In order to better understand these physico chemical behaviors, the structures of the obtained glasses were studied by Raman and NMR techniques. The rationale behind using NMR techniques was that these techniques allow structural characterization at the molecular level and are very sensitive to small variations in the chemical environment.

Raman Spectroscopy

Raman spectra of 40Na_2O-10SrO-(20-x)TiO_2-xSiO_2-30P_2O_5 glasses ($0 \leq x \leq 10$) glasses are shown in Fig. 6. As can be seen in Fig. 6, the bands are broad, which reflects the disordered structure of glasses, and were located at 400-600, 630-800, 800-1100, and 1150 cm^{-1}. Table 2 gives Raman wavenumbers and their assignments. According to previous studies [29-31], the band at 1150 cm^{-1}, clearly in the spectra of compositions x = 6 and x = 10, can be assigned to the coupled vibrations of P-O and Si-O, stretching in the P-O-Si linkages, and to a (PO_2) symmetric stretching of the monophosphate group. The bands observed in the high energy region 800-1100 cm^{-1} are attributed to the symmetrical and asymmetrical vibrations of the PO_4, P_2O_7, and SiO_4 units [32,33]. The relatively sharp peak around 1020 cm^{-1} is due to $P_2O_7^{4-}$ diphosphate ions [34,35]. The strong band around 730 cm^{-1} observed in the crystalline titanyl oxyphosphate [36,37], in the glass systems TiO_2-SiO_2 [38], Na_2O-P_2O_5 [39], Na_2O-TiO_2-P_2O_5 [31], Na_2O-TiO_2-SiO_2 [40], and Na_2O-SiO_2-P_2O_5 [29], is assigned to the Ti-O, Si-O, and P-O vibrations in the Ti-O-Ti-O-, Si-O-Ti, Si-O-Si, P-O-Si, and P-O-P linkages. The bands observed between 400 and 600 cm^{-1} [30,41] are attributed to O-P-O, P-O-P, O-Si-O deformations (δ2 and δ4 PO_4 modes) and Ti-O vibrations of TiO_6 octahedra [25]. Thus, it can be concluded that Si^{4+} ions act as a network former in the glasses. Raman results indicated that the glasses were composed of tetrahedral PO_4 units and tetrahedral SiO_4 units with P-O-Si linkages and TiO_6 octahedra. The presence of

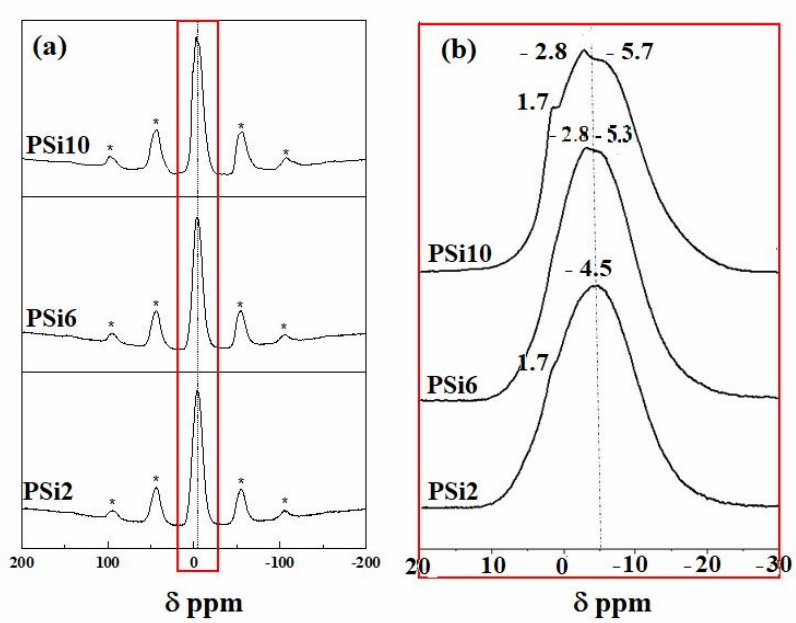

Fig. 7. (a) ^{31}P MAS NMR of $40Na_2O$-10SrO-(20-x)TiO_2-xSiO_2-$30P_2O_5$ glasses, (*) spinning sidebands; (b) ^{31}P NMR peak enlargement [x = 2: PSi2, x = 6: PSi6, x = 10: PSi10].

P-O-Si bonds, which are more ionic than P-O-P bonds, is in good agreement with the increase observed previously in the molar volume.

Solid-State ^{31}P NMR Spectroscopy

Figure 7a shows the ^{31}P MAS-NMR spectra of three studied glasses in the system $40Na_2O$-10SrO-(20-x)TiO_2-xSiO_2-$30P_2O_5$, with x = 2% (PSi2), 6% (PSi6), and 10% (PSi10) molar ratio. The spectra contained one isotropic chemical shift; this peak position varied between 20 and -30 ppm (Fig. 7b) while the remaining peaks, marked with asterisks, were spinning sidebands that deviated from magic-angle spinning. The ^{31}P MAS-NMR spectra (Fig. 7b) present an asymmetric and broad peak centered at -4.5 ppm for PSi2 glass with one shoulder at +1.7 ppm. For the PSi10 glass, containing 10% mol of SiO_2 oxide, in addition to the shoulder at +1.7 ppm, two signals were observed, one toward positive values from δ = - 4.5 ppm to δ = - 2.8 ppm and the other one toward negative values from δ = - 4.5 ppm to δ = - 5.7 ppm. Chemical shifts (δ) of the studied glasses corresponded to the resonance within the Q^1 region, *i.e.*, phosphorus atoms bonded to two BO atoms and two non-bridging oxygen (NBO) atoms [42]. The shoulder at δ = +1.7 ppm is attributed to the Q^1 region in phosphate glasses, with the atomic Na/P ratio slightly greater than one [43,44]. This was the case in the studied glasses where Na/P = 1.3. According to Fig. 7b, the center ^{31}P(Q^1) signal split into two peaks, with chemical shifts at -2.8 and -5.7 ppm, indicating that the introduction of silicon atoms changed the P environment and that these peaks were formed due to the phosphorus resonance in different sites. Previous studies have shown that the phosphorus chemical shift becomes more negative when the potential field of the nearest-neighboring cations z/ri (where z is the cation charge and ri is the ionic radius of the cation) increases [45,46]. Silicon was found to have a larger cation potential field (z/ri) than the other neighboring ions [z/r ($Å^{-1}$): Si^{4+} ~ 15, Ti^{4+} ~ 7, Sr^{2+} ~ 2, Na^+ ~ 1)]; thus, the chemical shift of P(Q^1) units in the vicinity of the silicon, compared to the units surrounded by titanium, sodium, and/or strontium, was characterized by a more negative chemical shift. Hence, the signal with the most negative value (at -5.7 ppm) can be attributed to the chemical displacement of P(Q^1) in P-O-Si bonds while the peak at δ = -2.8 ppm should be formed due to the chemical shift of P(Q^1) in P-O-M linkages, where M = Ti^{4+}, Sr^{2+}, Na^+ [26,46,47]. In

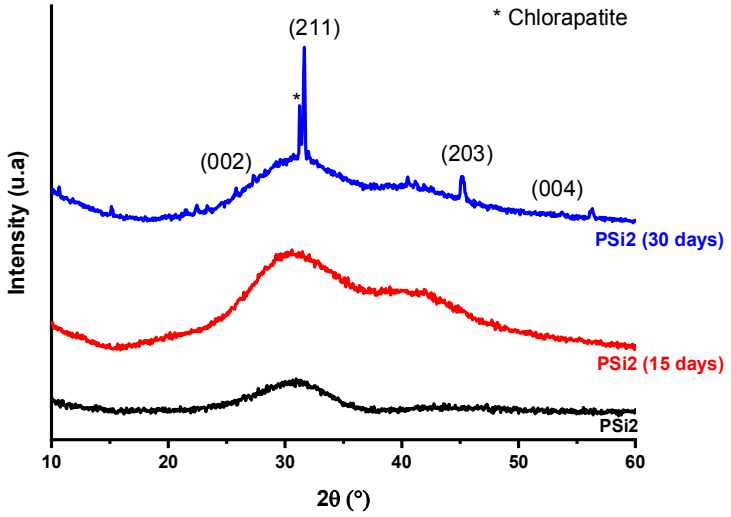

Fig. 8. XRD patterns of 40 Na_2O-10SrO-18TiO_2-2SiO_2-30P_2O_5 glass (PSi2) before and after immersion in SBF solution.

conclusion, ^{31}P MAS NMR study showed that Q^1 tetrahedra were the dominant P sites with the presence of P-O-Si linkages. This result confirms the results of Raman spectroscopy, which showed the formation of P-O-Si bonds when silicon was introduced into the phosphate glasses.

Bioactivity in Simulated Body Fluid (SBF)

The preliminary evaluation of *in vitro* bioactivity of 40Na_2O-10SrO-18TiO_2-2SiO_2-30P_2O_5 glass composition was carried out. XRD patterns of the studied glass before and after immersion in SBF solution for 15 and 30 days are presented in Fig. 8. The experimental XRD pattern shows the formation of both hydroxyapatite $Ca_5(PO_4)_3OH$ (HA) [ICSD file N°01-076-0694] and chlorapatite $Ca_5(PO_4)_3Cl$ (ClA) [ICSD file N°00-012-0263]. The formation of the apatite layer on the surface of the tested glass after immersion in SBF solution was confirmed with four diffraction maxima at 25.8, 31.6, 45.2, and 53.7° (2θ), which corresponded to the (0 0 2), (2 1 1), (2 0 3), and (0 0 4) apatite reflections, respectively [48]. The formation of chlorapatite was characterized by diffraction peaks at 31.2° and 32.2° (2θ). The presence of hydroxyapatite and chlorapatite was also confirmed by the appearance of infrared absorption bands, which are associated with the vibrations of P–O bonds in $(PO_4)^{3-}$ groups in HA and ClA (Fig. 9) [49,50]. The above results confirm the occurrence of ionic exchanges between the SBF solution and the studied glass by the precipitation of Ca-P layers on the surface of the studied glass.

CONCLUSIONS

The effect of the introduction of silicon oxide SiO_2 into the glasses with the molar compositions 40Na_2O-10SrO-(20-x)TiO_2-xSiO_2-30P_2O_5 ($0 \leq x \leq 10$) was evaluated using various techniques, such as density measurements, DSC, XRD, FTIR, Raman, and ^{31}P MAS NMR spectroscopies. The crystallization of the glasses led to the formation of a mixture of phases for all the glass compositions. The evolution of density, molar volume, and glass transition temperature (T_g) *versus* SiO_2 content suggests the weakening of the glass network due to the replacement of P-O-P bonds with the more ionic P-O-Si bonds. These results were confirmed by the Raman and ^{31}P MAS NMR spectroscopies. Raman spectroscopy also showed that the glasses contained PO_4, SiO_4 groups, short -O-Ti-O-Ti- chains, P-O-P, and P-O-Si linkages. Based on these results, it can be concluded that SiO_2 oxide, along with the P_2O_5 oxide, can act as a network former. In addition, the effect of the weakening of the glass network, caused due to the introduction of SiO_2, on the *in vitro* bioactivity was

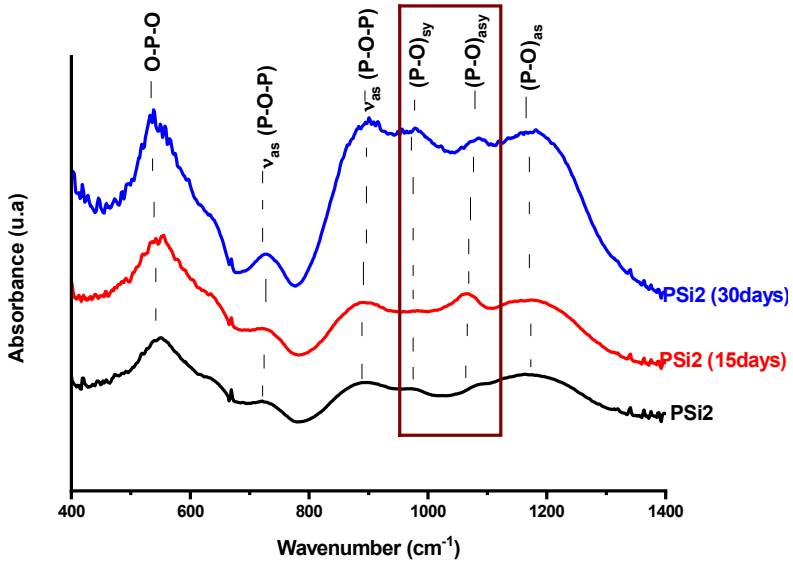

Fig. 9. FTIR spectra of 40 Na_2O-10SrO-18TiO_2-2SiO_2-30P_2O_5 glass (PSi2) before and after immersion in SBF solution.

assessed by the ability of the glasses to form Ca-P layers on their surfaces after immersion in SBF solution.

REFERENCES

[1] Minakshi, M.; Mitchell, D.; Jones, R.; Alenzazey, F., Synthesis, structural and electrochemical properties of sodium nickel phosphate for energy storage devices. *Nanoscale*. **2016**, *8*, 11291-11305, DOI: 10.1039/C6NR01179A.

[2] Rajendran, V.; Gayathri Devi, A. V.; Azooz, M.; El-Batal, F. H., Physicochemical studies of phosphate based P_2O_5-Na_2O-CaO-TiO_2 glasses for biomedical applications. *J. Non. Cryst. Solids*. **2007**, *353*, 77-84, DOI: 10.1016/j.jnoncrysol.2006.08.047.

[3] Lyczko, N.; Nzihou, A.; Sharrok, P., Calcium phosphate sorbent for environmental application. *Procedia. Eng.* **2014**, *83*, 423-431, DOI: 10.1016/j.proeng.2014.09.051.

[4] Serghini, A.; Brochu, R.; Ziyad, M.; Vedrine, J. C., Synthesis, characterization and catalytic behaviour of $Cu_{0.5}M_2(PO_4)_3$ (M Zr, Sn, Ti). *J. Alloys. Compd.* **1992**, *188*, 60-64, DOI: 10.1016/0925-8388(92)90643-N.

[5] Knowles, J. C., Phosphate based glasses for biomedical applications. *J. Mater. Chem.* **2003**, *13*, 2395-2401, DOI: 10.1039/b307119g.

[6] Abou Neel, E. A.; Pickup, D. M.; Valappil, S. P.; Newport, R. J.; Knowles, J. C., Bioactive functional materials: A perspective on phosphate-based glasses. *J. Mater. Chem.* **2009**, *19*, 690-701, DOI: 10.1039/b810675d.

[7] Sharmin, N.; Hasan, M. S.; Parsons, A. J.; Furniss, D.; Scotchford, C. A.; Ahmed, I.; Rudd, C. D., Effect of boron addition on the thermal, degradation, and cytocompatibility properties of phosphate-based glasses. *Biomed. Res. Int.* **2013**, *2013*, 1-12. DOI: 10.1155/2013/902427.

[8] Christie, J. K.; Ainsworth, R. I.; De Leeuw, N. H., Investigating structural features which control the dissolution of bioactive phosphate glasses: Beyond the network connectivity. *J. Non. Cryst. Solids.* **2016**, *432*, 31-34, DOI: 10.1016/ j.jnoncrysol.2015.01.016.

[9] Sharmin, N.; Rudd, C. D., Structure, thermal properties, dissolution behaviour and biomedical applications of phosphate glasses and fibres: A review. *J. Mater. Sci.* **2017**, *52*, 8733-8760, DOI: 10.1007/s10853-017-0784-4.

[10] Foroutan, F.; McGuire, J.; Gupta, P.; Nikolaou,

A.; Kyffin, B. A.; Kelly, N. L.; Hanna, J. V.; Gutierrez-Merino, J.; Knowles, J. C.; Baek, S. Y.; Velliou, E.; Carta, D., Antibacterial copper-doped calcium phosphate glasses for bone tissue regeneration, *Biomater. Sci. Eng*. **2019**, *5*, 6054-6062, DOI: 10.1021/acsbiomaterials.9b01291.

[11] Lusvardi, G.; Zaffe, D.; Menabue, L.; Bertoldi, C.; Malavasi, G.; Consolo, U., *In vitro* and *in vivo* behaviour of zinc-doped phosphosilicate glasses, *Acta Biomater*. **2009**, *5*, 419-428, DOI: 10.1016/j.actbio.2008.07.007.

[12] Hesaraki, S.; Gholami, M.; Vazehrad, S.; Shahrabi, S., The effect of Sr concentration on bioactivity and biocompatibility of sol-gel derived glasses based on CaO-SrO-SiO_2-P_2O_5 quaternary system. *Mater. Sci. Eng. C*. **2010**, *30*, 383-390, DOI: 10.1016/j.msec.2009.12.001.

[13] Parr, G. R.; Gardner, L. K.; Toth, R. W., Titanium: The mystery metal of implant dentistry. Dental materials aspects. *J. Prosthet. Dent*. **1985**, *54*, 410-414, DOI: 10.1016/0022-3913(85)90562-1.

[14] Brow, R. K., Review: the structure of simple phosphate glasses. *J. Non. Cryst. Solids*. **2000**, *263*, 1-28, DOI: 10.1016/S0022-3093(99)00620-1.

[15] Mošner, P.; Vosejpková, K.; Koudelka, L., Thermal behaviour and properties of Na_2O-TiO_2-P_2O_5 glasses. *J. Therm. Anal.* Calorim. **2009**, *96*, 469-474, DOI: 10.1007/s10973-008-9584-z.

[16] https://akjournals.com/view/journals/10973/96/2/article-p469.xml - affiliation0 [16] Abou Neel, E. A.; Chrzanowski, W.; Pickup, D. M.; O'Dell, L. A.; Mordan, N. J.; Newport, R. J.; Smith, M. E.; Knowles, J. C., Structure and properties of strontium-doped phosphate-based glasses. *J. R. Soc. Interface* **2009**, *6*, 435-446, DOI: 10.1098/rsif.2008.0348.

[17] Brauer, D. S.; Karpukhina, N.; Law, R. V.; Hill, R. G., Effect of TiO_2 addition on structure, solubility and crystallisation of phosphate invert glasses for biomedical applications. *J. Non. Cryst. Solids*. **2010**, *356*, 2626-2633, DOI: 10.1016/j.jnoncrysol.2010.03.022.

[18] Osipov, A. A.; Korinevskaya, G. G.; Osipova, L. M.; Muftakhov, V. A., Titanium coordination in TiO_2-Na_2O-SiO_2 glasses of $xTiO_2(100-X)$ [$2Na_2O$-$3SiO_2$] ($0 \leq x \leq 10$) composition based on Raman spectroscopy. *Glas. Phys. Chem*. **2012**, *38*, 357-360, DOI: 10.1134/S1087659612040098.

[19] Yarker, C. A.; Johnson, P. A. V.; Wright, A. C.; Wong, J.; Greegor, R. B.; Lytle, F. W.; Sinclair, R. N., Neutron diffraction and exafs evidence for TiO_5 units in vitreous $K_2O.TiO_2.2SiO_2$. *J. Non. Cryst. Solids*. **1986**, *79*, 117-136, DOI: 10.1016/0022-3093(86)90041-4.

[20] Lakhkar, N.; Abou Neel, E. A.; Salih, V.; Knowles, J. C., Titanium and strontium-doped phosphate glasses as vehicles for strontium ion delivery to cells. *J. Biomater. Appl.* **2011**, *25*, 877-893, DOI: 10.1177/0885328210362125.

[21] Shah Mohammadi, M.; Ahmed, I.; Muja, N.; Rudd, C. D.; Bureau, M. N.; Nazhat, S. N., Effect of phosphate-based glass fibre surface properties on thermally produced poly(lactic acid) matrix composites. *J. Mater. Sci. Mater. Med*. **2011**, *22*, 2659-2672, DOI: 10.1007/s10856-011-4453-x.

[22] Aldaadaa, A.; Al Qaysi, M.; Georgiou, G.; M. A.; Leeson, R.; Knowles, J. C., Physical properties and biocompatibility effects of doping SiO_2 and TiO_2 into phosphate-based glass for bone tissue engineering. *J. Biomater. Appl.* **2018**, *33*, 271-280, DOI: 10.1177/0885328218788832.

[23] Said, H.; Oueslati Omrani, R.; Arana, L. R.; El Bahri, D.; Boussen, S.; Bouzidi, C.; Terraschke, H.; Hamzaoui, A. H.; M'nif, A., The effect of silica additive on the structural and luminescence properties of Eu^{3+}/Tb^{3+} co-doped metaphosphate glasses. *J. Mol. Struct.* **2019**, *1192*, 42-48, DOI: 10.1016/j.molstruc.2019.04.087.

[24] Kokubo, T.; Kushitani, H.; Sakka, S.; Kitsugi, T.; and Yamamum, T., Solutions able to reproduce in vivo surface-structure changes in bioactive glass-ceramic A-W3. *J. Biomed. Mater. Res.* **1990**, *24*, 721-734, DOI: 10.1002/jbm.820240607.

[25] Tiwari, B.; Pandey, M.; Sudarsan, V.; Deb, S. K.; and Kothiyal, G. P., Study of structural modification of sodium aluminophosphate glasses with TiO_2 addition through Raman and NMR spectroscopy. *Phys. B Condens. Matter*. **2009**, 404, 47-51,

DOI: 10.1016/j.physb.2008.10.016.

[26] Kaoua, S.; Krimi, S.; El Jazouli, A.; Hlil, E. K.; Waal, D., Preparation and characterization of phosphate glasses containing titanium and vanadium. *J. Alloys Compd.* **2007**, *429*, 276-279, DOI: 10.1016/j.jallcom.2006.04.004.

[27] Lamrhari, S.; El Khalidi, Z.; Krimi, S.; Haddad, M.; Couzi, M.; Lachgar, A.; El Jazouli, A., Synthesis and structural characterization of phosphate-based Nasiglasses $Na_3Ca1\text{-}x\ MnxTi(PO_4)_3(0 \leq x \leq 10)$. *J. Mater. Environ. Sci.* **2018**, *9*, 3009-3018. http://www.jmaterenvironsci.com.

[28] Mooghari, H. R. A.; Nemati, A.; Yekta, B. E.; Hamnabard, Z., The effects of SiO_2 and K_2O on glass forming ability and structure of $CaO\text{-}TiO_2\text{-}P_2O_5$ glass system. *Ceram. Int.* **2012**, *38*, 3281-3290, DOI: 10.1016/j.ceramint.2011.12.034.

[29] Chakraborty, I. N.; and Condrate, R. A., the vibrational spectra of glasses in the $Na_2O\text{-}SiO_2\text{-}P_2O_5$ system with a 1:1 SiO_2:P_2O_5 molar ratio. *Phys. Chem. Glas.* **1985**, *26*, 68-73, https://www.researchgate.net/publication/275973126

[30] Shibata, N.; Horigudhi, M.; Edahiro, T., Raman spectra of binary high-silica glasses and fibers containing GeO_2, P_2O_5 and B_2O_3. *J. Non. Cryst. Solids.* **1981**, *45*, 115-126, DOI: 10.1016/0022-3093(81)90096-X.

[31] Krimi, S.; El Jazouli, A.; Rabardel, L.; Couzi, M.; Mansouri, I.; Le Flem, G., Glass formation in the $Na_2O\text{-}TiO_2\text{-}P_2O_5$ System. *J. Solid State Chem.* **1993**, *102*, 400-407, DOI: 10.1006/jssc.1993.1051.

[32] Karakassides, M. A.; Saranti, A.; Koutselas, I., Preparation and structural study of binary phosphate glasses with high calcium and/or magnesium content. *J. Non. Cryst. Solids.* 2004, *347*, 69-79, DOI: 10.1016/j.jnoncrysol.2004.08.111.

[33] Kalampounias, A. G., IR and Raman spectroscopic studies of sol-gel derived alkaline-earth. *B. Mater. Sci.* **2011**, *34*, 299-303, DOI: 10.1007/s12034-011-0064-x.

[34] Cornilsen, B. C.; Condrate, R. A., The vibrational spectra of α-alkaline earth pyrophosphates. *J. Solid State Chem.* **1978**, *23*, 375-382, DOI: 10.1016/0022-4596(78)90087-7.

[35] Philip, D.; George, B. L.; Aruldha, G., IR and polarized Raman spectra of $Na_4P_2O_7{\cdot}10H_2O$. *J. Raman Spectrosc.* **1990**, *21*, 523-524, DOI: 10.1002/jrs.1250210810.

[36] Bamberger, C. E.; and Begun, G. M., Synthesis and characterization of titanium phosphates, TiP_2O_7 and $(TiO)_2P_2O_7$. *J. Less Common Metals.* **1987**, *134*, 201-206, DOI: 10.1016/0022-5088(87)90558-3.

[37] Bamberger, C. E.; Begun, G. M.; and Cavin, O. B., Synthesis and characterization of sodium-titanium phosphates, $Na_4(TiO)(PO_4)_2$, $Na(TiO)PO_4$, and $NaTi_2(PO_4)_3$. *J. Solid State. Chem.* **1988**, *73*, 317-324, DOI: 10.1016/0022-4596(88)90115-6.

[38] Best, M. F.; Condrate, R. A., A raman study of TiO_2-SiO_2 glasses prepared by sol-gel processes. *J. Mater. Sci. Lett.* **1985**, *4*, 994-998, DOI: 10.1007/BF00721102.

[39] Sridarane, R.; Raje, G.; Shanmukaraj, D.; Kalaiselvi, B. J.; Santhi, M.; Subramanian, S.; Mohan, S.; Palanivel, B.; Murugan, R., Investigations on temperature defendant structural evolution of $NaPO_3$ glass. *J. Therm. Anal. Calorim.* **2004**, *75*, 169-178, DOI: 10.1023/ b:jtan.0000017339.26217.db.

[40] Scannell, G.; Barra, S.; Huang, L., Structure and properties of $Na_2O\text{-}TiO_2\text{-}SiO_2$ glasses: Role of Na and Ti on modifying the silica network. *J. Non. Cryst. Solids.* **2016**, *448*, 52-61, DOI: 10.1016/j.jnoncrysol.2016.06.028.

[41] Avadhesh, K. Y.; Singha, P., A review of structure of oxide glasses by raman spectroscopy avadhesh. *RSC Adv.* **2015**, *5*, 67583-67609, DOI: 10.1039/C5RA13043C.

[42] Kirkpatrick, R. J.; Brow, R. K., Nuclear magnetic resonance investigation of the structures of phosphate and phosphate-containing glasses: A review, *J. Solid. State. Nucl. Magn. Reson.* **1995**, *5*, 9-21, DOI: 10.1016/0926-2040(95)00042-O.

[43] Brow, R. K.; Kirkpatrick, R.J., Turner, G.L., The short range structure of sodium phosphate glasses I. MAS NMR studies. *J. Non. Cryst. Solids.* **1990**, *116*, 39-45, DOI: 10.1016/0022-3093(90)91043-Q.

[44] Montagne, L.; Palavit, G.; Delaval, R., 31P NMR in $(100\text{-}x)(NaPO_3)$-xZnO glasses, *J. Non. Cryst. Solids.* **1997**, *215*, 1-10, DOI: 10.1016/S0022-3093(97)00032-X.

[45] Turner, G. L.; Smith, K. A.; Kirkpatrick, R. J.; Oldfield, E., Structure and cation effects on phosphorus-31PMASNMR chemical shifts and chemical-shift anisotropies of orthophosphates. *J. Magn. Reson.* **1986**, *70*, 408 -415, DOI: 10.1016/0022-2364(86)90129-0.

[46] Brow, R. K.; Phifer, C. C.; Turner, G. L.; Kirkpatrick, R. J., Cation effects on 31P MAS NMR chemical shifts of metaphosphate glasses. *J. Am. Ceram. Soc.* **1991**, *74*, 1287-1290, DOI: 10.1111/ j.1151-2916.1991.tb04099.x.

[47] Pires, R.; Abrahams, I.; Nunes, T. G.; Hawkes, G. E., Non-random cation distribution in sodium-strontium-phosphate glasses. *J. Non. Cryst. Solids.* **2004**, *337*, 1-8, DOI: 10.1016/ j.jnoncrysol.2004.03.108.

[48] Dietrich, E.; Oudadesse, H.; Lucas-Girot, A.; Le Gal, Y.; Jeanne, S.; Cathelineau, G., Effects of Mg and Zn on the surface of doped melt-derived glass for biomaterials applications. *Appl. Surf. Sci.* **2008**, *255*, 391-395, DOI: 10.1016/j.apsusc.2008.06.094.

[49] Ashok, M.; Meenakshi Sundaram, N.; and Narayana Kalkura, S., Crystallization of hydroxyapatite at physiological temperature. *Mater. Lett.* **2003**, *57*, 2066-2070, DOI: 10.1016/S0167-577X(02)01140-0.

[50] Wan, J.; Zhang, C.; Zeng, G.; Huang, D.; Hu, L.; Huang, C.; Wu, H.; Wang, L., Synthesis and evaluation of a new class of stabilized nano-chlorapatite for Pb immobilization in sediment, *J. Hazard. Mater.* **2016**, *320*, 278-288. Doi.org/10.1016/j.jhazmat.2016.08.038.